Electrochimica Acta 213 (2016) 14–20

Contents lists available at ScienceDirect

Electrochimica Acta

journal homepage: www.elsevier.com/locate/electacta

Self-Organization Process of Aluminum Oxide during Hard Anodization

Juan Li[a,*], Zhiying Zhang[a], Yuxin Li[a], Yingjun Ma[a,b], Lin Chen[a], Zhongyue Zhang[a], Runguang Sun[a,*]

[a] School of Physics and Information Technology, Shaanxi Normal University, Xi'an, 710119, PR China
[b] School of Science, Ningxia Medical University, Yinchuan, 750004, PR China

ARTICLE INFO

Article history:
Received 14 March 2016
Received in revised form 7 June 2016
Accepted 7 June 2016
Available online 8 June 2016

Keywords:
Porous anodic alumina
hard anodization
self-organization
pore rearrangement
unequilibrium process

ABSTRACT

The self-organization process of the porous anodic alumina (PAA) during hard anodization (HA) was proposed by synthetically investigating the nanopore morphology, the current density and barrier layer evolution of the PAA films, which were anodized in 0.3 M oxalic acid at 150 V (the voltage rising from 40 V to 150 V at the beginning). It was found that the high enough current density in the voltage rising stage can induce the fast film growth, which caused the pores to rapidly enlarge themselves and to reach a relatively ordered rearrangement. The barrier layer thickness showed linearly increase in voltage rising stage and then increased with a decelerated speed in the followed constant anodization stage, where the pores with growth advantage moved down straightly and gradually expanded their cell size to replace the inferior pores around. Accordingly, HA is a unequilibrium process and can be divided into two stages: I, the rapid pore enlargement and rearrangement during voltage rising stage, where the oxidation rate is larger than that of dissolution; II, competing growth of the nanopores during the followed constant voltage anodization, where the oxidation and dissolution rates approach to each other due to the thickened barrier layer. These findings are very helpful for more efficiently controlling the hard anodization process and developing new electrolyte systems to further broaden the interpore distance range.

1. Introduction

After nearly two decades of development, self-organized porous anodic alumina (PAA) has become one of the most popular templates to prepare various functional ordered nanostructures (*e.g.*, nanorods, nanotubes and nanocones) made up of metal, inorganic and polymer materials, which have demonstrated unique optic, electric and magnetic properties [1–6]. Moreover, PAA itself is also a versatile platform to develop novel chemical and biological sensors [7], energy storage devices [8], drug delivery systems [9], and so on. It has many advantages in stability, low-cost, operating convenience and technique compatibility. However, in typical two-step mild anodization processes, hexagonally packed nanopores with fixed interpore distance (D_{int}) of 63 nm, 100 nm and 500 nm can only be obtained in the three corresponding processing windows: sulphuric acid (H_2SO_4) at 25 V, oxalic acid ($H_2C_2O_4$) at 40 V, and phosphoric acid (H_3PO_4) at 195 V [10–12]. And the first anodization, which consumes several hours, is proved to be an important factor to influence the order of the PAA films. Recently, hard anodization (HA) characterized by the high current density has attracted highly attention, which is an efficient and inexpensive method not only to get long-rang ordered PAA films in short time but also to achieve different D_{int} from typical mild anodization. Many efforts have been made to find new self-ordering regime of PAA by exploring the compatible electrolyte systems and anodization voltage [13–17]. To date, highly ordered nanopores with continuously tunable D_{int} in the range of 70–490 nm have been successfully achieved by HA in the precisely chosen electrolyte systems and under the corresponding anodization voltages [15,16]. However, few works concern about the nature of the HA processes. It is still a puzzle that how the nanopores adjust themselves to form the high-ordered arrangement during the HA.

During a typical HA process, both the voltage and current show their characteristic variations. Anodization voltage step-wise increases from a low value to the high target value, and the current density shows a nearly exponential decrease as a function of time in the constant voltage anodization stage. It was widely accepted that the nearly exponential decreased current was caused by the gradually decreased concentration of anions along the

* Corresponding authors. Tel.: +86 29 8153 0826; fax: +86 29 8153 0826.
E-mail addresses: jli2007@snnu.edy.cn (J. Li), sunrunguang@snnu.edu.cn (R. Sun).

http://dx.doi.org/10.1016/j.electacta.2016.06.044
0013-4686/

nanopores due to the "diffusion limited effect" [13,18,19]. And little attention have been paid on the influence of the voltage rising stage on HA [19,20]. According to the high field conductivity theory, it can be deduced that the change of the voltage and current in HA will cause the variation of local electric field, which will make the corresponding changes of the arrangement and geometric parameters of nanopores. Furthermore, the changes of arrangement and geometric parameters of nanopores would in turn affect the current variation. However, the arrangement and geometric parameters evolution of nanopores under the effect of changed voltage and current is still unclear. In fact, knowing the self-organization process of the nanopores during in HA is very essential for understanding the growth mechanism of the nanopores, which is also very helpful for controlling the anodization process efficiently and further broadening the D_{int} range.

In this paper, we have demonstrated that the self-organization process of the nanopore in HA was a unequilibrium process that the dissolution and the generation rates of the aluminum oxide were not equally to each other by synthetically investigating the nanopore morphology, the current density and barrier layer evolution during the whole HA process in 0.3 M oxalic acid at U = 150 V. Firstly, highly enough dissolution and oxidation rates needed to be reached in the voltage rising stage so as to generate strong mechanical stress to obtain the relatively ordered rearrangement of the nanopores, where the oxidation rate was larger than that of dissolution. Secondly, the pores with growth advantage can gradually enlarge themselves to replace the pores with defects in the following constant voltage anodization, where the arrangement of the nanopores became more and more order; the barrier layers thickened with a deceleration speed and the propagation rate of oxide/metal (o/m) interface and electrolyte/oxide (e/o) interface approached to each other equally, which in mainly responded for the nearly exponential decreased current. At last, high-ordered arranged nanopores were fabricated in large area by using the HA technology.

2. Experimental

2.1. Reagents and Materials

Highly pure (99.999%) aluminum disks with a thickness of 0.2 mm and diameters of 35 mm and 100 mm were used as starting materials (Cuibolin Nonferrous Metals Co., Ltd, Bejing, China). Analytical reagents were produced by Tianjing TianLi Chemical

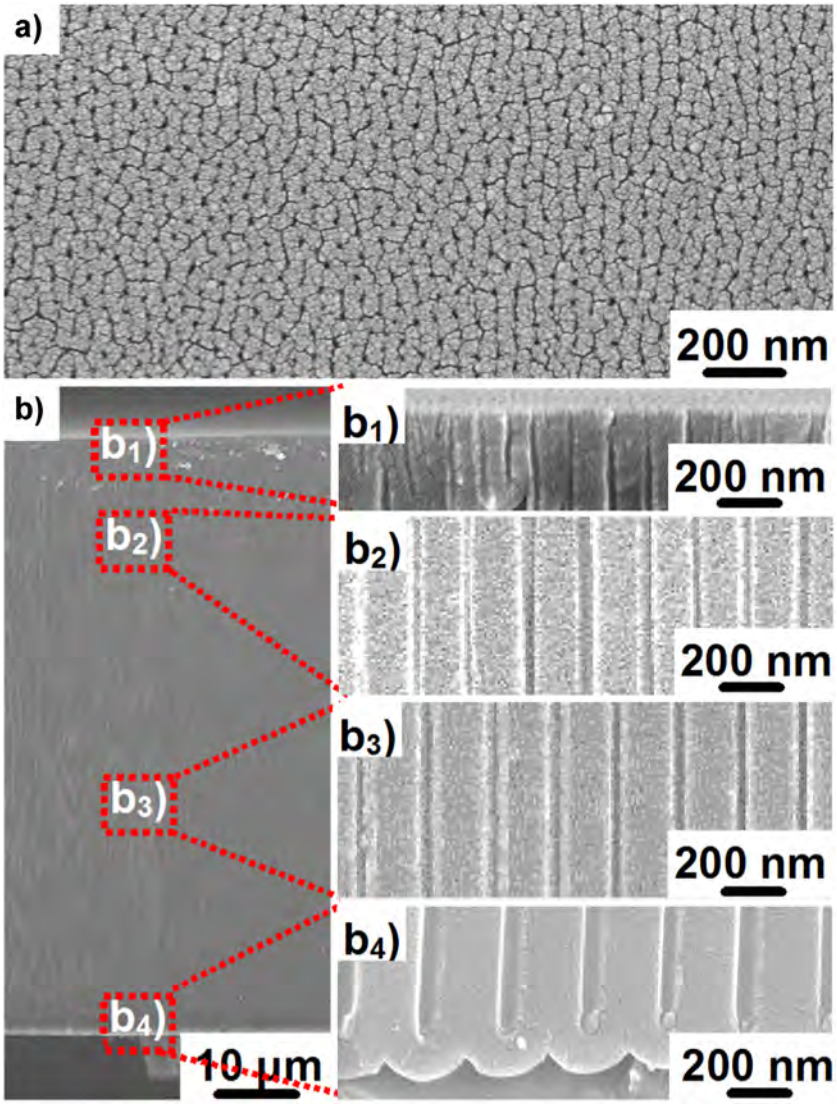

Fig. 1. SEM top view (a) and side view (b) of the PAA film that was formed in hard anodization in 0.3 M oxalic acid for 5500s. b_1)-b_4) show four different parts of the PAA film from top down.

Reagents Ltd (China), including oxalic acid dihydrate ($C_2H_2O_4{\cdot}2H_2O$, 99.5 wt%), sulfuric acid (H_2SO_4, 98 wt%), phosphoric acid (H_3PO_4, 85 wt%), chromium trioxide (CrO_3, 99 wt%), perchloric acid ($HClO_4$, 70–72 wt%), ethanol (CH_3CH_2OH, 99.7 wt%). The de-ionized water was produced by a pure water system.

2.2. Hard anodization

Al disks were firstly electropolished in a mixture of perchloric acid and ethanol (V/V = 1:4) for 8 min (20 V, 0 °C). The electropolished disk was then placed in a custom-tailored electrochemical cell equipped with a circle cooling system (DC-3006, Ningbo Scientz Biotechnology Co., Ltd), where the cooling liquid (ethanol) can remove the reaction heat from both the back of Al foils and electrolyte. The circle reaction zone exposed to the electrolyte was 25 mm or 85 mm in diameter. A platinum electrode was employed as a counter electrode, and the electrolyte solution were under violent agitation. As the electrolyte is 0.3 M oxalic acid, the anodization firstly proceeded at 40 V for 8 min, and then the voltage was gradually increased to the target value of 150 V at the rate of 0.5 V s^{-1}. As the electrolyte is the mixture of 0.3 M oxalic acid and 0.012 M sulfuric acid, the anodization firstly proceeded at 35 V for 8 min, and then the voltage was gradually increased to the target value of 110 V. The temperature was kept at 0–1 °C. Current densities (j) were calculated by dividing the current values measured from the power supply system (IT 6874A, ITECH) by the anodized sample area. After the anodization, the as-prepared nanosamples were immersed into a mixed solution of 1.8 wt% CrO_3 and 6 wt% H_3PO_4 for 6 h at 65 °C to peel off the alumina films to obtain the corresponding nanodents.

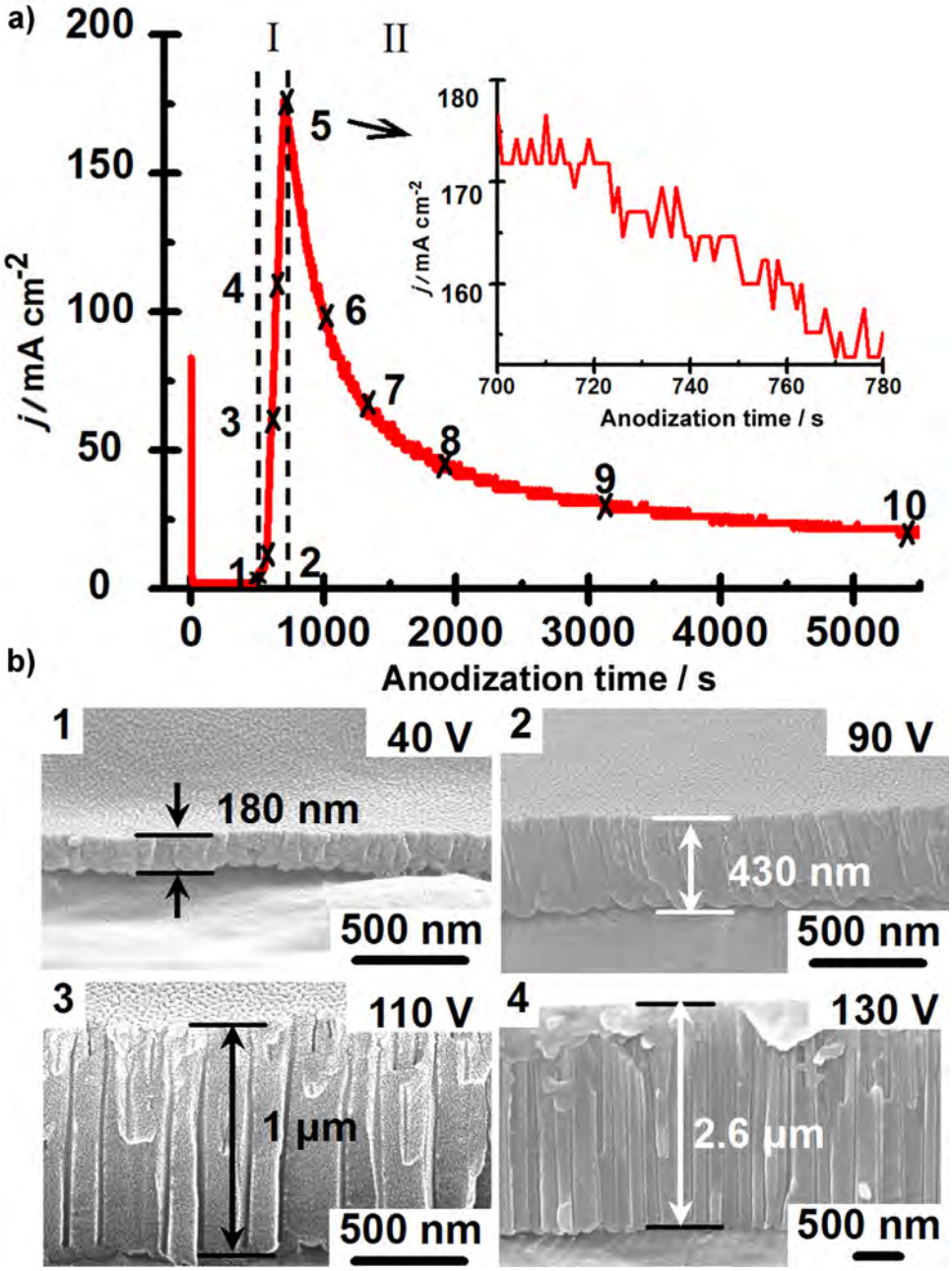

Fig. 2. (a) The evolution of current density (j) as a function of anodization time. The whole hard anodization can be divided into two stages: I, voltage rising stage; II, constant voltage anodization, where the j decreases after reach the maxima (the insert). (b) Side views of PAA films formed at different time in the stage I.

2.3. Structure characterization

The geometrical morphologies of all samples were observed under a field-emission scanning electron microscope (FE-SEM, Nova NanoSEM 450, FEI) after sputtering a 15-nm thickness of Au layer. To obtain the morphology parameters of the nanopores, we generally observed five batches of samples and at least twenty pores per sample under high-resolution scanning electronic microscope.

3. Results and Discussion

3.1. Nanopore morphology evolution during hard anodization

To explore the overall variation trend of the nanopores during HA, morphology scrutiny was carried out by analyzing the SEM top-views and side-views of different places along the vertical direction of the exemplified porous alumina films, which was obtained by HA in 0.3 M oxalic acid. The electropolished highly

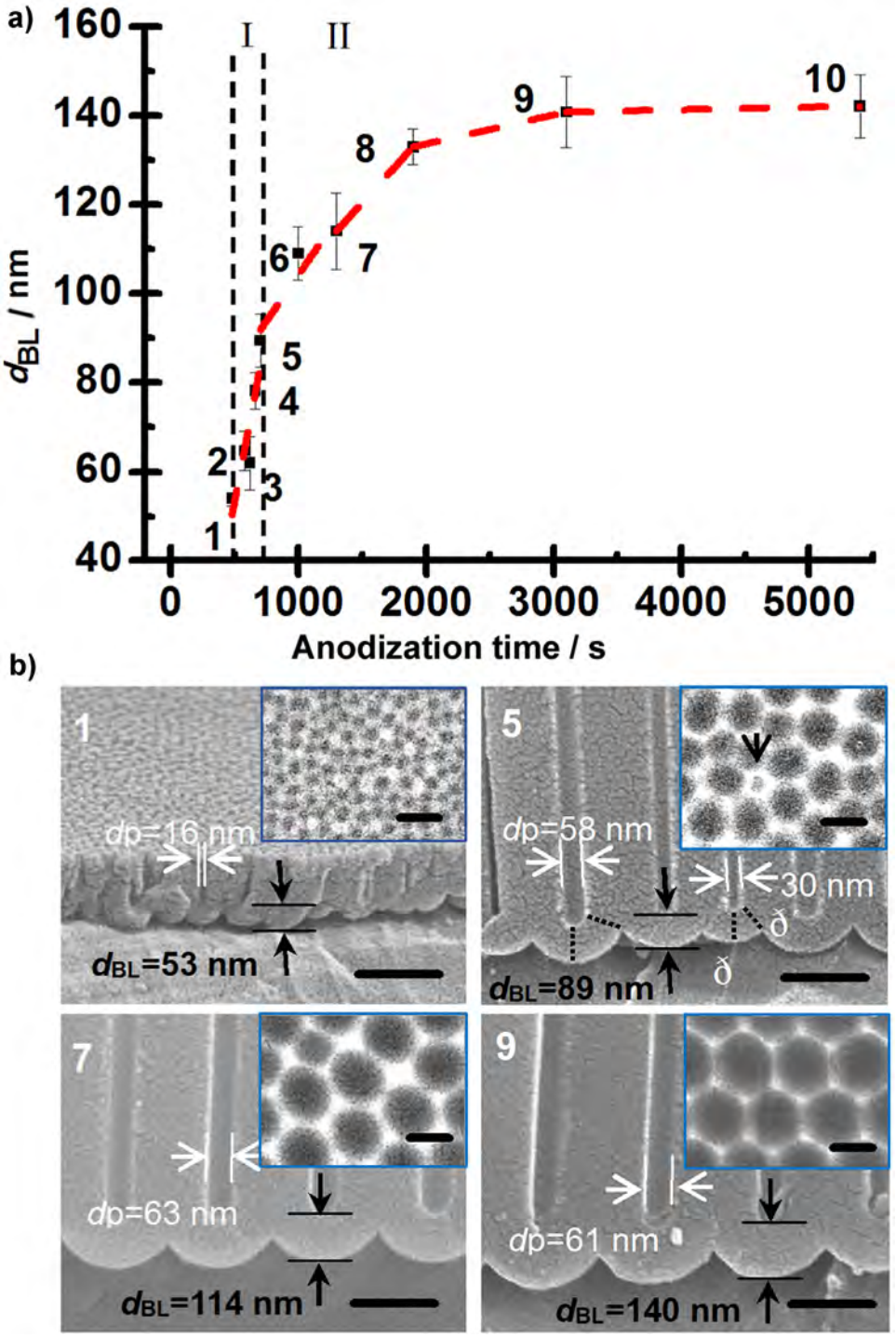

Fig. 3. (a) Barrier layer thickness (d_{BL}) as a function of time during HA. (b) Structural details of barrier layer under different anodization time. The inserts show the SEM top-views of the nanodents that obtained by peeling off the corresponding PAA films. ð′ and ð in b5 represent the oxide thickness along the ridge-top and the oxide thickness along the pore axis, respectively. The black arrow in the insert of b5 shows the defect of nanodents. The scar bar is 200 nm.

pure (99.999%) aluminum foils were first mild anodized at 40 V for 8 min to form the protective layer, and then the voltage stepwise increased to $U = 150$ V at the rate of 0.5 V s^{-1}. The anodization temperature always kept at 0–1 °C by a circle cooling system, and the total anodization time was 5500 s [15]. As shown in Fig. 1a, many tiny nanopores and cracks cover the whole sample surface, which arise from the concentration of the electric field in the initial mild anodization stage [21]. The average pore diameter (d_p) and D_{int} are only 13 ± 1 nm and 55 ± 1 nm, respectively. The whole cross section of the as-prepared film with total thickness of ca.110 μm was shown in Fig. 1b, and its morphology details of different parts were shown in Fig. 1b1–b4. It can be seen that, at the early anodization stage (Fig. b1 and b2), the pore channels are not very straight due to the variation of the pore diameter and their sizes are also different with each other. As the anodization prolongs, the pore channels become more and more regular (Fig. 1b3 and b4). Another interesting phenomenon should be paid attention to that D_{int} also become larger from Fig. 1b1 to b4, which suggests that lots of the nanopores should cease their growth during the anodization. However, it is very hard to directly observe the termination of individual nanopore and measure the enlargement of D_{int} from the cross section of the film, because the breakage of the PAA film is a random event, and the as-prepared film is too thick to ensure the cleavage plane always go through the center of one pore from top down.

3.2. Current density evolution during hard anodization

To have a deep insight of the structural evolution of the PAA films, we have monitored the current density variation during the whole anodization process, as shown in Fig. 2a. Here the Arabic numbers of 1, 2, 3, 4, 5, 6, 7, 8, 9, 10 that marked on the graph stand for anodization time of 480 s (40 V), 580 s (90 V), 620 s (110 V), 660 s (130 V), 700 s (150 V), 1000 s (150 V), 1300 s (150 V), 1900s (150 V), 3100s (150 V) and 5400s (150 V), respectively. According to the anodization, we divide the whole hard anodization process into two parts after the pre-mild anodization treatment: I, from 1 to 5 (480–700 s), j increases to the peak value of 177 mA/cm^2, which stands for that the voltage slowly increased from 40 V to 150 V at the rate of 0.5 V/s; II, after 5, j shows an oscillatory and nearly exponential decrease as a function of time, which stands for that the constant voltage anodization process at 150 V. j almost reaches to a plateau of 19 mA/cm^2 after point 10. Interestingly, during stage I, though the voltage arise rate is the same, the increase speed of j between 2 to 5 is obviously larger than 1 to 2, which means the different growth rate of the PAA film.

It is believed that the rapid oxide formation due to the high current density is the key factor to obtain the highly ordered arrangement of the nanopores [13]. Accordingly, we measured the PAA film thickness at different points in the voltage rising stage, as shown in Fig. 2b. It is found that the growth rate of the PAA film shows an accelerating increment in stage I. The average growth rate increases from 2.6 nm/s (from 1 to 2) up to 16 nm/s (from 2 to 3), then to 40 nm/s (from 3 to 4). Note that, the growth rate begins to accelerate after point 2 due to the enhanced electric field caused by increased voltage, which corresponds to the current density variation very well. Such high growth rate certainly leads to the quick rearrangement of the nanopores. It had been reported that long-range ordered nanopores can only be obtained above 110 V (i.e. 120–150 V) in HA in pure oxalic acid system [13,15]. Combined with our experiment, we can deduce that the oxide growth rate needs reaching a high enough value (>16 nm/s in this situation) in the voltage rising stage so as to generate strong mechanical stress at the o/m interface, which leads to form a rearrangement that allows certain nanopores to competitively grow in the constant voltage anodization and reach the highly ordered arrangement at last.

3.3. Barrier layer evolution during hard anodization

It is well known that the anodization current is mainly related to the movement of ionic species through the barrier layer, and the logarithm of the current density is inversely dependent on the thickness of the barrier layer (d_{BL}) [22]. To understand the variation trend of current and prove our hypothesis, we in detail investigated into the barrier layer as a function of time (t) during the whole anodization process, as shown in Fig. 3. By carefully measuring d_{BL} of the PAA films under different anodization time, it is found that d_{BL} increases with respect to reaction time, and the increment becomes more and more smaller in stage II and almost closes to zero after 9 (Fig. 3a). It should be noted that d_{BL} increment in stage I is obviously faster than stage II, but there is almost no change from 2 to 3.

It is easily to understand that the step raised anodization voltage will cause the stronger effective electric field strength (E), which can generate stronger force to drive the oxygen anions through the oxide film and simultaneously lead to more severe polarization and impairment of the Al-O bond of alumina [22]. Thus, both generation and dissolution rate of alumina are enhanced and result in the faster growth of the film. However, the oxidation rate is greater than the dissolution rate of the oxide [22], which makes the propagation rate of o/m interface larger than that of e/o interface and results in the d_{BL} thickening. Apparently, the variation of the barrier layer has hysteretic nature. As the electric field strength increases to the value of point 2, the film has achieved the rapid growth (i.e. the rapid increment of the current) owning to the untimely thickened barrier layer. After that, d_{BL} keeps on thickening to reduce the E. Thus, once the voltage has reached the constant value, the current presents the exponential decrease and the barrier layer thickens with a decelerated speed, which means the movement of o/m interface and e/o interface are approaching to each other. Note that, d_{BL} almost has no variation after 9, but the current density still decreases from 31 mA cm^2 (9) to 19 mA cm^2 (10), this may be ascribed to the extended diffusion path of the acid anions along the nanopores.

It should be pointed out that D_{int} and d_p also changed. The insert of Fig. 3b shows several representive nanodents images, which were obtained by peeling off the corresponding PAA films. The relatively ordered nanodents array can be already achieved at the end of the stage I due to the fast growth of the nanopores (Fig. 3b5). Although there are many defects (black arrow in the insert), most of the nanodents show the hexagonally packed, which is corresponding to our expectation. As the anodization time prolongs, the arrangement of the nanodents is improved obviously as the D_{int} increasing, which average values are 83 nm (1), 180 nm (5), 274 nm (7) and 320 nm (9), respectively. In order to comprehend such variation trend, we carefully investigated the bottom of the corresponding nanopores. It can be seen that, compared with mild anodization (Fig. 3b1), both d_p and d_{BL} dramatically increase at the end of stage I (Fig. 3b5) due to the enhanced dissolution and generation rates of the oxide. However, the increments are not evenly. Certain pores have smaller d_{BL} and d_p than others (Fig. 3b5), which makes the ratio between the oxide thickness along the ridge-top (Ð×) and the oxide thickness along the pore axis (Ð) becomes larger. This morphology can effectively reduce E and thus result in the slow growth speed of the pores [23]. Besides, although d_{BL} become thicker, d_p of the pores almost have no change in the constant voltage anodization (Fig. 3b5–b9). As a result, the pores with growth advantage move down straightly and gradually expand themselves to replace the inferior pores around,

and form the highly ordered arrangement at last by the competitive growth.

3.4. Self-organization process of nanopores during hard anodization

Accordingly, we can divide the HA process into two stages (Fig. 4a): I, the rapid rearrangement stage during voltage rising. In this stage, about half of the nanopores formed in the pre-mild anodization cease their growth, while the left dramatically enlarge their period and pore diameter to reach a relatively ordered arrangement due to the high enough growth speed. However, the enlargement is not equally to each pores, and lots of defects generate in this stage; II, Competing growth of nanopores during constant voltage anodization. In this stage, the oxidation and dissolution rate move closer to the balance point along the anodization time. And the pores with growth advantage move down straightly and gradually expand the cell size, and replace the inferior pores around, where the defects were repaired and the pore arrangement become more and more regular. It should be noted here that: 1) to obtain the highly-ordered arrangement of the nanopore at last, it is essential to reach a highly enough film growth speed in the voltage rising step. For example, long-range ordered nanopores can be obtained at 110 V only by adding tiny amount sulfuric acid in the oxalic acid solution to increase the peak current density (i.e. growth rate), while the nanopores will lose their order at 150 V by adding ethanol due to the decreased current density [15]. 2) The self-organization of the nanopore is a process that needs to be performed at low and stable temperature. Thus, it is very important to ensure the effective heat dissipation during the whole anodization process. The local heat accumulation will accelerate the film dissolution speed, which prevent the barrier layer to thicken and result in the burnt event. The anodization can be performed intervallic so as to guarantee the effective heat dissipation. For example, using intervallic anodization technology, highly-ordered nanodents with period of 220 nm (Fig. 4c) on a large Al disc with diameter of 85 mm (Fig. 4b) can be obtained by anodizing in the mixture of 0.3 M oxalic acid and 0.012 M sulfuric acid. These findings are very helpful for more efficiently controlling the HA process and developing new electrolyte system to further broaden the D_{int} range, which have wide application in fabricating optimized functional materials.

4. Conclusions

We have demonstrated that the self-organization process of the porous anodic alumina during hard anodization is a unequilibrium process that the dissolution and the generation rate of the aluminum oxide are not equal to each other. By synthetically investigating the nanopore morphology, the current density and barrier layer evolution, we divided the whole process into two stages: I, the rapid pore enlargement and rearrangement during voltage rising stage, where the oxidation rate is larger than that of dissolution; II, competing growth of the nanopores during the followed constant voltage anodization, where the pores with growth advantage move down straightly and gradually expand their cell size to replace the inferior pores around. The oxidation and dissolution rates approach to each other due to the thickened barrier layer in stage II, where arrangement of the nanopores

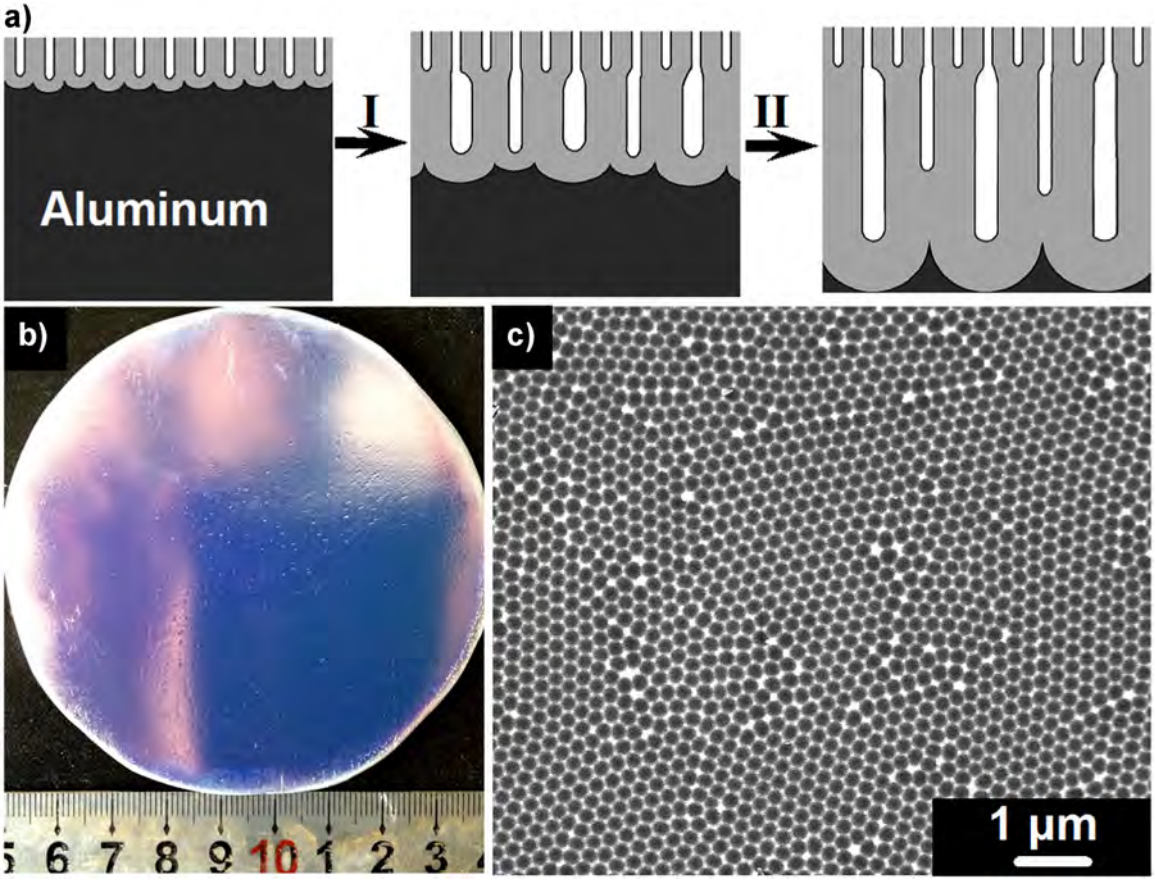

Fig. 4. (a) A schematic describes the self-organization process of porous anodic alumina during HA (Not to scale). I: the rapid rearrangement of nanopores during voltage rising stage. II: Competing growth of nanopores during constant voltage anodization. (b) A photograph shows a Al disc with diameter of 85 mm that is patterned with nanodents with D_{int} of 220 nm by HA. (c) SEM images of the nanodents on (b).

becomes more and more order. These findings are very helpful for controlling the hard anodization process efficiently and developing new electrolyte system to further broaden the interpore distance range.

ACKNOWLEDGMENT

This work was supported by the National Natural Science Foundation of China (201403285), Natural Science Foundation of Jiangsu Province (BK20130355), Fundamental Research Funds for the Central Universities (GK201603019, GK201601008) and Scientific Research Foundation of Shaanxi Normal University.

References

[1] W. Lee, S.-J. Park, Porous anodic aluminum oxide: anodization and templated synthesis of functional nanostructures, Chem. Rev. 114 (2014) 7487.
[2] Y. Lei, W. Cai, G. Wilde, Highly ordered nanostructures with tunable size, shape and properties: A new way to surface nano-patterning using unltra-thin alumina masks, Prog. Mater. Sci. 52 (2007) 465.
[3] J. Li, L. Hu, C. Li, X. Gao, Tailoring hexagonally packed metal hollow-nanocones and taper-nanotubes by template-induced preferential electrodeposition, ACS Appl. Mater. Interfaces 5 (2013) 10376.
[4] Y. Yamauchi, T. Nagaura, A. Ishikawa, T. Chikyow, S. Inoue, Evolution of standing mesochannels on porous anodic alumina substrates with designed conical holes, J. Am. Chem. Soc. 130 (2008) 10165.
[5] S. Grimm, R. Giesa, K. Sklarek, A. Langner, U. Gösele, H.-W. Schmidt, M. Steinhart, Nondestructive replication of self-ordered nanoporous alumina membranes via cross-linked polyacrylate nanofiber arrays, Nano Lett. 8 (2008) 1954.
[6] J. Li, J. Zhu, X. Gao, Bio-inspired high-performance antireflection and antifogging polymer films, Small 10 (2014) 2578.
[7] A. Santos, T. Kumeria, D. Losic, Nanoporous anodic alumina: A versatile platform for optical biosensors, Materials 7 (2014) 4297.
[8] P. Banerjee, I. Perez, L. Henn-Lecordier, S.B. Lee, G.W. Rubloff, Nanotubular metal-insulator-metal capacitor arrays for energy storage, Nat. Nanotech. 4 (2009) 292.
[9] G. Jeon, S.Y. Yang, J.K. Kim, Functional nanoporous membranes for drug delivery, J. Mater. Chem. 22 (2012) 14814.
[10] H. Masuda, K. Fukuda, Ordered metal nanohole arrays made by a two-step replication of honeycomb structures of anodic alumina, Science 268 (1995) 1466.
[11] H. Masuda, K. Yada, A. Osaka, Self-ordering of cell configuration of anodic porous alumina with large-size pores in phosphoric acid solution, Jpn. J. Appl. Phys. 37 (1998) L1340.
[12] A.P. Li, F. Müller, A. Birner, K. Nielsch, U. Gösele, Hexagonal pore arrays with a 50-420 nm interpore distance formed by self-organizatioin in anodic alumina, J. Appl. Phys. 84 (1998) 6023.
[13] W. Lee, R. Ji, U. Gösele, K. Nielsch, Fast fabrication of long-range ordered porous alumina membranes by hard anodization, Nat. Mater. 5 (2006) 741.
[14] S. Ono, M. Saito, H. Asoh, Self-ordering of anodic porous alumina formed in organic acid electrolytes, Electrochim. Acta 51 (2005) 827.
[15] J. Li, C. Li, C. Chen, Q. Hao, Z. Wang, J. Zhu, X. Gao, Facile Method for Modulating the Profiles and Periods of Self-ordered three-dimensional alumina taper-nanopores, ACS Appl. Mater. Interfaces 4 (2012) 5678.
[16] B. Sun, J. Li, X. Jin, C. Zhou, Q. Hao, X. Gao, Self-ordered hard anodization in malonic acid and its application in tailoring alumina taper-nanopores with continuously tunable periods in the range of 290–490 nm, Electrochim. Acta 112 (2013) 327.
[17] Y. Li, Y. Qin, S. Jin, X. Hu, Z. Ling, Q. Liu, J. Liao, C. Chen, Y. Shen, L. Jin, A new self-ordering regime for fast production of long-range ordered porous anodic aluminum oxide film, Electrochim. Acta 178 (2015) 11.
[18] Y. Li, Z. Ling, X. Hu, Y. Liu, Y. Chang, Investigation of intrinsic mechanisms of aluminium anodization processes by analyzing the current density, RCS Adv. 2 (2012) 5164.
[19] A. Santos, J.M. Montero-Moreno, J. Bachmann, K. Nielsch, P. Formentín, J. Ferré-Borrull, J. Pallarès, L.F. Marsal, Understanding pore rearrangement during mild to hard transition in bilayered porous anodic alumina membranes, ACS Appl. Mater. Interfaces 3 (2011) 1925.
[20] Z. He, M. Zheng, M. Hao, T. Zhou, L. Ma, W. Shen, Evolution process of orderly nanoporous alumina by constant high field anodization in oxalic acid electrolyte, Appl. Phys. A 104 (2011) 89.
[21] G.E. Thompson, Porous anodic alumina: fabrication, characterization and applications, Thin Solid Films 297 (1997) 192.
[22] Z. Su, G. Hähner, W. Zhou, Investigation of the pore formation in anodic aluminium oxide, J. Mater. Chem. 18 (2008) 5787.
[23] J.E. Houser, K.R. Hebert, Modeling the potential distribution in porous anodic alumina films during steady-state growth, J. Electrochem. Soc. 153 (2006) B566.